3D+t segmentation of PET images using spectral clustering

Hiba Zbib, Salam Kdouh, Sandrine Mouysset, Simon Stute, Jean-Marc Girault, Jamal Charara, Mohammad Nassereddme, Ali Mcheik, Irene Buvat, Clovis Tauber

3D+t segmentation of PET images using spectral Clustering

Hiba Zbib[*‡], Salam kdouh[*], Sandrine Mouysset[†], Simon Stute[§], Jean-Marc Girault[‡], Jamal Charara[*], Mohammad Nassereddine[*], Ali Mcheik[*], Irène Buvat[§] and Clovis Tauber[‡]
*Laboratoire Signaux et Images, Université Libanaise, Al Hadath, Liban
‡UMRS INSERM U930 - Université de Tours Hopital Bretonneau, France
†CNRS UMR 5055 – Université de Toulouse
§IMIV, UMR 1023 Inserm/CEA/Université Paris Sud, ERL 9218 CNRS, CEA SHFJ, Orsay, France
Email: hibazbib@hotmail.com, clovis.tauber@univ-tours.fr

***Abstract*— Segmentation of dynamic PET images is often needed to extract the time activity curve (TAC) of regions. While clustering methods have been proposed to segment the PET sequence, they are generally either sensitive to initial conditions or favor convex shaped clusters. Recently, we have proposed a deterministic and automatic spectral clustering method (AD-KSC) of PET images. It has the advantage of handling clusters with arbitrary shape in the space in which they are identified. While improved results were obtained with AD-KSC compared to other methods, its use for clinical applications is constrained to 2D+t PET data due to its computational complexity. In this paper, we propose an extension of AD-KSC to make it applicable to 3D+t PET data. First, a preprocessing step based on a recursive principle component analysis and a Global K-means approach is used to generate many small seed clusters. AD-KSC is then applied on the generated clusters to obtain the final partition of the data. We validated the method with GATE Monte Carlo simulations of Zubal head phantom. The proposed approach improved the region of interest (ROI) definition and outperformed the K-means algorithm.**

I. INTRODUCTION

Dynamic PET image segmentation is needed to extract the time activity curves (TAC) of regions of interest. These TAC can be used in compartmental models for in vivo quantification of the radiotracer target. The regions in which TAC are calculated are usually delineated manually by operators. These manual delineations are time consuming and subjective due to noise and poor spatial resolution of PET images. As a result, there is a growing interest in the development of clustering methods that aim at separating the PET image into functional regions. Wong et al. [1] proposed to segment dynamic PET images using a K-means algorithm. Parker et al. [2] proposed a graph-based method for the minimization of Mumford-Shah energy in order to estimate the input function directly from the carotid artery. After preprocessing the data with principal component analysis, their method used the Mahalanobis distance as similarity measure. Recently, an Automatic and Deterministic Kinetic Spectral Clustering (AD-KSC) method that has the advantage of handling arbitrary shaped clusters in the space in which they are identified was proposed [3]. Spectral clustering involves the eigendecomposition of a pairwise Laplacian matrix in order to define a low-dimensional space in which data points can be clustered [3], [4]. While improved results were obtained with AD-KSC compared to other methods, its use for clinical applications is still constrained to 2D+t PET data due to the computation complexity of the dominant eigenvectors. However, it is important to consider the entire 3D sequence, and segment it to similar functional volume. This improves the statistical robustness compared to 2D segmentation to obtain a smooth representation of each region. To make it applicable in 3D, a preprocessing step reducing the size of the data clustered is applied to PET data. Several authors proposed approaches to deal with large datasets. Chaoji et al. [6] have proposed a method that handles full-dimensional, arbitrary shaped clusters. Their SPARCL method consists first on running a carefully initialized version of the K-means algorithm to generate many small seed clusters then iteratively merges the generated clusters. Guo et al. [7] presented a method that combines a pre-clustering process using a histogram based thresholding with a hierarchical cluster analysis. They have extended their method to make it adapted for 3D PET data. They integrated a clustering slice by slice with a hierarchical clustering technique. In this paper, we propose a method ADKSC-3D, inspired from Guo et al. [7], Chaoji et al. [6] and Zbib et al. [3] in which a preprocessing step using a principal component analysis and a clustering with the Global K-means approach is applied slice by slice on the initial TACs. As a result, many small seed clusters are generated. Then AD-KSC-3D is applied on the reduced data to obtain the final partition. To validate our approach, GATE Monte Carlo simulations of the Zubal head phantom were performed. The AD-KSC-3D was evaluated on this simulated phantom and favorably compared to the K-means approach.

II. THE PROPOSED AD-KSC-3D METHOD

A. Notation

Let us T denote the number of frames contained in the PET sequence, K the number of functional regions of the 3D PET volume, $x_i \in \mathbb{R}^T$ the mean TAC of voxels belonging to the same region i calculated by the preprocessing step.

B. Preprocessing step for each slice

The preprocessing step aims to reduce the size of the data extracted from each slice. The preprocessing step consists of:

- Determination of axis with maximal variance with principal component analysis: the covariance matrix

Fig. 1. Regions of the Zubal head phantom used for image simulation.

- is calculated and the eigenvector that corresponds to the highest eigenvalue is determined. The data are projected on this axis.
- Clustering the projected data by Global K-means (GKM): the projected data are separated into two sub groups using the Global K-means approach (GKM) [8]. This approach has the advantage of being fast and deterministic. The algorithm continues recursively on each sub groups and the recursion usually terminates when the resulting clusters contain a number of point b less than a prespecified value (called bucket size).
- Label computation of each voxel: the centers of the generated regions are calculated and the Euclidian distance between all voxels TAC and the generated centers are computed. Each voxel is then affected to the nearest center.
- Construction of a matrix A containing the average TACs $x_i \in \mathbb{R}^T$ for each region.

C. *Clustering of the generated regions by AD-KSC*

The representative TAC of the generated regions for each slice are calculated and denoted x_i . They are grouped to form the matrix A which is used as input for the AD-KSC algorithm. By using the preprocessing step, the size of PET data is considerably reduced. This allows the application of AD-KSC on 3D PET data. The AD-KSC can be summarized by 5 steps as described below [10]:

1) Mapping the data into high dimensional space: The similarities between all pairs of x_i are calculated using a Gaussian kernel function to project the data into a high dimensional space. The entries of the similarity matrix are calculated as:

$$S(x_i, x_j) = \frac{-d(x_i,x_j)^2}{2\sigma^2} \quad (1)$$

where S(x_i , x_j) is the similarity between the TACs of regions i and j, σ is a scale parameter that is a threshold which adjusts the distance of patterns mapped into the feature space, and d(x_i , x_j) is a weighted Euclidean distance that we defined as:

$$d(x_i, x_j) = \sum_{t=1}^{T} w_t \left((x_i(t) - x_j(t))^2\right)^{1/2} \quad (2)$$

In this work the weight of each frame is set equal, so that all frames have the same contribution. This weight can be varied as a function of the frame for radiotracers that are only separable in earlier noisy frames.

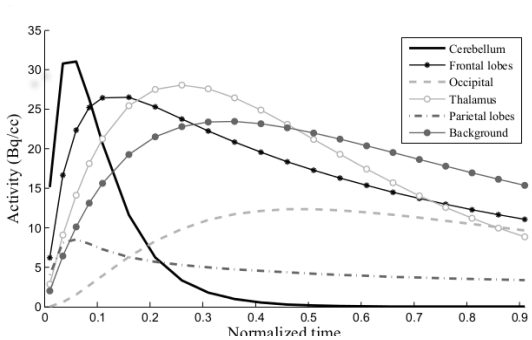

Fig. 2. TACs used to simulate the dynamic PET series.

2) Projection into low dimensional space: A Laplacian random walk matrix denoted L_{rw} is derived from the similarity information. Spectral clustering using L_{rw} can be interpreted as trying to find a partition of the graph such as the random walk stays long within the same cluster and seldom jumps between clusters. The K dominant eigenvectors of L_{rw} are used to project the data on a reduced space where the natural clusters in the data become more linearly separable.

3) Deteministic search for centroids in feature space: In AD-KSC we proposed to use a Global K-means approach[8] to classify the projected data in the last step of spectral clustering method. The Global K-means is an incremental approach that dynamically adds one cluster center at a time. Unlike the K-means algorithm (KM), the GKM algorithm always starts from the same centers, which are iteratively selected from the data itself, in order to obtain deterministic clustering of the data. The clustering process of AD-KSC is therefore deterministic, which is a necessary condition for the global optimization of its parameters. To reduce the time needed for convergence we used the fast Global K means proposed by [8].

4) Unsupervised normalized minimal distance criterion: In the segmentation of dynamic PET images, two phenomena frequently occur: the separation and the fusion of clusters. To detect these two phenomena, several unsupervised criteria were proposed. Dunn [10] proposed a cluster validity index to identify compact and well separated clusters, and defined the diameter of a cluster as the maximal intra cluster distance between all pairs of points. In [3], we proposed a criterion that consists in a robust extension of the Dunn index. We defined the normalized minimal distance (NMD) criterion as:

$$NMD = -\frac{\delta_{min}}{\Delta_{max}^{95}} \quad (3)$$

where δ_{min} is a minimal inter-cluster distance that decreases when voxels representing similar time courses are assigned to different clusters. It is defined as follows:

$$\delta_{min} = \min_{1 \le o \le p \le K} \| C_o - C_p \| \quad (4)$$

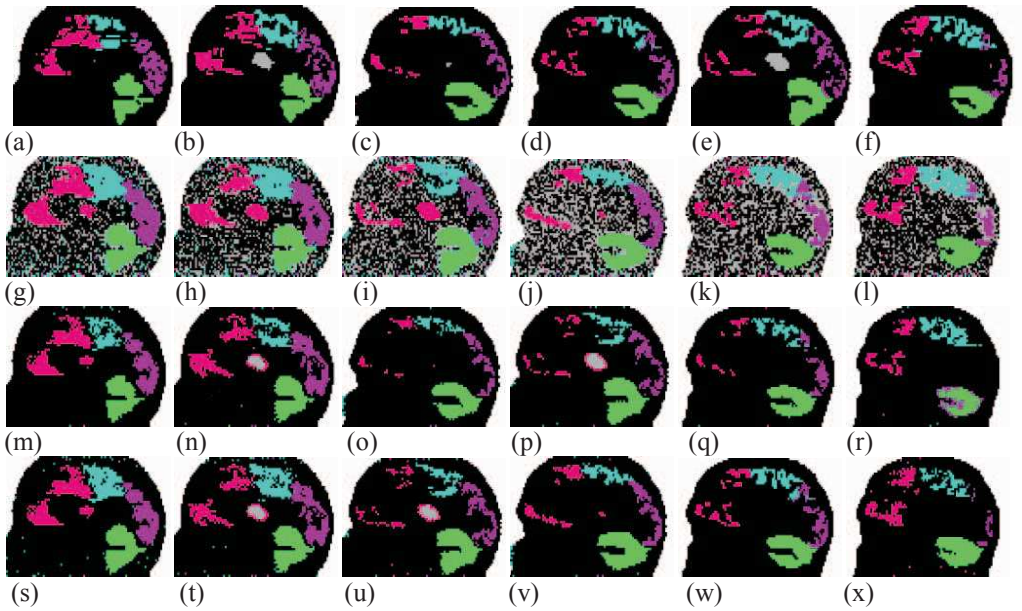

Fig. 3. Sagittal views of the results obtained with KM and AD-KSC on each slice and AD-KSC-3D. First row: sagittal view of the ground truth images used for comparison: (a) slice 131, (b) slice 133, (c) slice 136, (d) slice 140, (e) slice 143, (f) slice 145. Second row: sagittal view of the results obtained with KM: (g) slice 131, (h) slice 133, (i) slice 136, (j) slice 140, (k) slice 143, (l) slice 145. Third row: sagittal view of the results obtained with AD-KSC applied on each slice: (m) slice 131, (n) slice 133, (o) slice 136, (p) slice 140, (q) slice 143, (r) slice 145. fourth row: sagittal view of the results obtained with AD-KSC-3D: (s) slice 131, (t) slice 133, (u) slice 136, (v) slice 140, (w) slice 143, (x) slice 145.

TABLE I. PFOM CALCULATED FOR THE AD-KSC AND AD-KSC-3D APPROACHES ON 6 SLICES.

	131	**133**	**136**	**140**	**143**	**145**
AD-KSC	0.96	0.95	0.90	0.90	0.86	0.85
AD-KSC-3D	0.94	0.97	0.95	0.99	0.96	0.94

where C_o and C_p are the centers of cluster G_o and G_p respectively and $\|C_o - C_p\|$ is the Euclidean distance between these two centers. Δ_{max}^{95} is a robust maximal intra-cluster distance that tends to increase when a fusion of clusters occurs. It is defined as:

$$\Delta_{max}^{95} = \max_{1 \le l \le K} \frac{\sum_{x_i x_j \in G_l} \|x_i - x_j\| A(\|x_i - x_j\| \ge dl_{95th})}{N_l \times 0.05} \quad (5)$$

where $dl_{95^{th}}$ is the 95 percentile of intra cluster distances of cluster G_Z, N_z is the number of voxels belonging to G_Z and A is a Boolean function such that A(Y) = 1 if Y is true and 0 otherwise. The proposed NMD criterion increases when a fusion or a splitting of clusters occurs.

5) Global optimization of NMD by simulated annealing: In [3], we proposed to estimate automatically the scale parameter involved in the similarity matrix by a global optimization scheme using the simulated annealing algorithm. At each iteration, the scale parameter of AD-KSC is randomly perturbed and the NMD cost function is calculated. Downhill steps are always accepted while uphill steps are accepted to step out of a local minimum under a probability acceptance function [3].

III. VALIDATION OF AD-KSC-3D ALGORITHM

A. Simulation of realistic PET images

We performed GATE Monte Carlo simulations of Gemini GXL PET 4D acquisitions. The labeled MR image of the Zubal head phantom was used as voxelized sources of $1.1 \times 1.1 \times 1.4\ mm^3$ (figure 1). The regional TACs (figure 2) were generated according to the three-compartment model as proposed by Maroy et al. [11]. We used six regions of the Zubal head phantom: the cerebellum, the thalamus, the frontal, occipital, parietal lobes and the remaining parts of the head (called background) plus a seventh region with no activity corresponding to the air around the head. These regions constituted the ground truth for evaluation of the results. This sequence consisted of 5×30s followed by 15 × 60s dynamic frames. The reconstruction of the dynamic PET images was performed with an ANW-OSEM iterative method, using four iterations and 16 subsets, into voxels of 2.2 mm × 2.2 mm × 2.8 mm.

B. Quantitative evaluation of the results

The quality of segmentation results was assessed using two supervised criteria: Pratt's Figure of Merit (PFOM) [12] that measures the precision of edge locations in the 3D segmented images, compared to their ground truth locations and Adjusted Rand Index (ARI) [13] that evaluates the consistency between ground truth regions and those of the segmented images. These two supervised criteria have values between 0 and 1. When the segmented results perfectly agree with the ground truth, these criteria are equal to 1.

TABLE II. CONVERGENCE TIME AND QUANTITATIVE CRITERIA CALCULATED FOR THE K-MEANS APPROACH

	PFOM	ARI	Time
KM	0.43	0.74	3.22 min

TABLE III. CONVERGENCE TIME AND QUANTITATIVE CRITERIA CALCULATED FOR DIFFERENT BUCKET SIZE.

Bucket size (b)	ARI	PFOM	Time
30	0.84	0.97	22 min
50	0.84	0.97	11 min
100	0.83	0.96	5 min
250	0.77	0.92	3.5 min
300	0.77	0.91	3.4 min
400	0.73	0.87	0.87 min

IV. RESULTS

A. Evaluation of AD-KSC-3D for different bucket size

Different bucket size were tested: 30, 50, 100, 250, 300 and 400 and the segmentation quality of the proposed AD-KSC-3D was evaluated. Table III presents the quantitative ARI and PFOM criteria and the convergence time needed for each value. ARI and PFOM were found constant for a bucket size
smaller than 100, but they decrease when the bucket size increases. This can be due to the fusion of different regions on the preprocessing step. The convergence time is greater when the bucket size is smaller because the size of data clustered by the AD-KSC is bigger. Generally, a bucket size smaller than 100 can be used to obtain good segmentation quality with an acceptable convergence time.

B. Comparison between K-means, AD-KSC and AD-KSC-3D

AD-KSC-3D is compared with the K-means approach [1] and AD-KSC applied on each 2D slice [3]. The K-means starts from a random initialization of the centers and iteratively finds the partition of data that minimizes their distances to the clusters centroids. The figure 3 displays representative results of the clustering obtained with KM, AD-KSC and AD-KSC-3D algorithms. The first row in figure 3 displays the ground truth of six slices selected from the segmented 3D images. Figure 3(g-l) display representative results of the clustering obtained with the KM algorithm. The KM merges the frontal lobe with the thalamus (Fig.3(h,i)) and the background is separated into two parts (Fig.3(g-l)). Figure 3(m-r) presents the results of AD-KSC applied on each 2D slice without preprocessing. The results are similar to the AD-KSC-3D for most slices, but for slice 145 (figure 3 (r)) the occipital lobe is merged with the background and the cerebellum is separated into two regions. Figure 3(s-x) display representative results of the clustering obtained with the AD-KSC-3D algorithm. Generally all regions are properly identified and the number of cluster is correctly detected in each slice. This is a good feature of the algorithm because it is not necessary to have a priori knowledge on the number of regions contained in each slice. Table I presents the PFOM calculated for the slices segmented by AD-KSC and AD-KSC-3D. PFOM shows an improvement of the definition of functional regions. Table II presents the quantitative ARI, PFOM criteria and the convergence time needed for the KM algorithm. ARI and PFOM are smaller than the criteria calculated with AD-KSC-3D for different bucket sizes as shown in table III. Compared to KM, AD-KSC-3D using a bucket size of 300 has the same convergence time with higher quantitative criteria as shown in tables III,II.

V. CONCLUSION

A preprocessing step based on a recursive principal component analysis and a Global K-means approach is applied to generate many small clusters for each slice. The clusters means are calculated and used as representative of each region. AD-KSC is then applied on the generated cluster means in order to obtain the final partition of the 3D PET data. In our experiments, the AD-KSC-3D results improved the identifiability of functional regions and outperformed AD-KSC applied on 2D slices and the K-means approach.

REFERENCES

[1] K.-P. Wong, D. Feng, S. Meikle, and J. Fulham, "Segmentation of Dynamic PET Images Using Cluster Analysis." IEEE Trans. NucL. Sci., vol. 49, pp. 200–207, 2002.

[2] B. J. Parker and D. D. Feng, "Graph-Based MumfordShah Segmentation of Dynamic PET With Application to Input Function Estimation," IEEE Trans. NucL. Sci., vol. 52, pp. 79–89, 2005.

[3] H. Zbib, S. Mouysset, S. Stute, J. Girault, J. Charara, S. Chalon,L. Galineau, I. Buvat, and C. Tauber, "Unsupervised spectral clustering for segmentation of dynamic PET images," IEEE Trans. NucL. Sci.,vol. PP, 2015. DOI: 10.1109/TNS.2015.2399973.

[4] U. Luxburg, "A tutorial on Spectral Clustering." Statistics and computing, vol. 17, pp. 395–416, 2007.

[5] S. Mouysset, H. Zbib, S. Stute, J. Girault, J. Charara, J. Noailles, I. Buvat, and C. Tauber, "Segmentation of dynamic PET images with kinetic spectral clustering," Phys. Med. Biol., vol. 58, pp. 6931–6944, 2013.

[6] V. Chaoji, M. Hasan, S. Salem, and M. J. Zaki, "Sparcl: an effective and efficient algorithm for mining arbitrary shape-based clusters." Knowl. Inf. Syst., vol. 21, pp. 201–229, 2009.

[7] H. Guo, R. Renault, K. Chen, and E. Reiman, "Clustering huge data sets for parametric PET imaging." Biosystems, vol. 71, pp. 81–92, 2003.

[8] A. Likas, N. Vlassis, and J. J. Verbeek, "The Global K-means clustering algorithm," Pattern Recognition, vol. 36, pp. 451–461, 2003.

[9] H. Zbib, S. Mouysset, S. Stute, J. Girault, J. Charara, S. Chalon, L. Galineau, I. Buvat, and C. Tauber, "Deterministic spectral clustering for segmentation of dynamic PET imaging," in J. Nucl. Med., 2012.

[10] J. C. Dunn, "A fuzzy relative of the isodata process and its use in the detecting compact well-separated clusters," Journal of Cybernetics, vol. 3, pp. 32–57, 1973.

[11] R. Maroy, R. Boisgard, C. Comtat, V. Frouin, P. Cathier, E. Duchesnay, F. Dolle, P. E. Nielsen, R. Trebossen, and B. Tavitian, "Segmentation of rodent whole-body dynamic PET images: an unsupervised method based on voxel dynamics." IEEE Trans. Med. Imag., vol. 27, pp. 342–354, 2008.

[12] W. Pratt, Digital Image Processing. Wiley, 1977.

[13] W. M. Rand, "Objective criteria for the evaluation of clustering method," Journal of the American Statistical Association, vol. 66, pp. 846–850, 1971.